

Asynchronous Distributed Voltage Control in Active Distribution Networks

Zhaojian Wang^a, Feng Liu^{a,*}, Yifan Su^a, Boyu Qin^b

^aState Key Laboratory of Power Systems, Department of Electrical Engineering, Tsinghua University, Beijing 100084, China

^bState Key Laboratory of Electrical Insulation and Power Equipment, School of Electrical Engineering, Xi'an Jiaotong University, Xi'an 710049, China

Abstract

With the explosion of distributed energy resources (DERs), voltage regulation in distribution networks has been facing a great challenge. This paper derives an asynchronous distributed voltage control strategy based on the partial primal-dual gradient algorithm, where both active and reactive controllable power of DERs are considered. Different types of asynchrony due to imperfect communication or practical limits, such as random time delays and non-identical sampling/control rates, are fitted into a unified analytic framework. The asynchronous algorithm is then converted into a fixed-point problem by employing the operator splitting method, which leads to a convergence proof with mild conditions. Moreover, an online implementation method is provided to make the controller adjustable to time-varying environments. Finally, numerical experiments are carried out on a rudimentary 8-bus system and the IEEE-123 distribution network to verify the effectiveness of the proposed method.

Keywords: Distributed control, distribution networks, (partial) primal-dual gradient algorithm, asynchronous algorithm, voltage control

1. Introduction

With the proliferation of distributed energy resources (DERs), such as small hydro plants, Photovoltaics (PVs) and energy storage systems, voltage regulation in active distribution networks is greatly challenged. On the one hand, the voltage quality remarkably degrades, e.g., the voltage may fluctuate rapidly due to the variation of renewable generations and over-voltage exists at the buses DERs connected. On the other hand, many DERs, such as some small hydro plants Han et al. (2014) and inverter-integrated DERs Turitsyn et al. (2011), have great potential of voltage regulation by appropriately managing their active or reactive power outputs. Beyond the capability of traditional voltage regulation schemes, these challenges call for a new voltage control paradigm.

The voltage control in a distribution network aims to minimize the voltage mismatch by regulating active or reactive power outputs of controllable DERs. Generally speaking, it can be viewed as a type of optimal power flow (OPF) problems, where the branch power flow model is usually utilized Baran and Wu (1989a,b). Similar topics have been studied extensively in the literature. Related works can roughly be categorized into three classes in terms of the communication requirements: centralized control, local control and distributed control. In the centralized voltage control, a global optimization problem is formulated and solved by a central controller to determine optimal set-points for the overall system Farivar et al. (2011, 2012); Kekatos et al. (2015a). In this case, the central controller collects all the required information and communicates with all

DERs. However, it suffers from the single-point-failure issue and costs long computation time when the number of DERs is large. As for the local voltage control, locally available information such as bus voltage magnitude is utilized to design the controller Turitsyn et al. (2011). In the problem formulation, the linearized distribution power flow is usually utilized, and the objective function is a specific form Zhu and Liu (2016); Liu et al. (2017); Zhou et al. (2018). As it uses only local information, the response is rapid. However, the control objective is restricted to specific types, making it less flexible. The distributed voltage control can avoid the disadvantages of centralized and local controls to some extent Antoniadou-Plytaria et al. (2017). Compared with the centralized control, there is no central controller and communication is usually between immediate neighbors Šulc et al. (2014); Bolognani et al. (2015); Zhang et al. (2015); Liu et al. (2018a,b) or two-hop neighbors Tang et al. (2019). Compared with the local voltage control, the objective function can be more general and practical. In existing literature, the distributed voltage control is usually synchronous. However, asynchrony widely exists in power systems, such as communication time delay caused by congestion or even failure and different sampling or computation rates. In the synchronous case, the slowest bus and communication channel may cripple the system Peng et al. (2016); Yi and Pavel (2019a).

This paper designs an asynchronous distributed strategy for voltage control in distribution networks. Various types of asynchrony in power systems are considered, such as communication delay, and different sampling rates, which are fitted into a unified framework. This is different from Bolognani et al. (2015), which only considers asynchronous iterations and assumes no communication delay. The proposed method is also different from the asynchronous control in Zhu and Liu (2016),

^{*}This work was supported by the National Natural Science Foundation of China (No. 51677100, U1766206, No. 51621065).

^{*}Corresponding author

Email address: lfeng@mail.tsinghua.edu.cn (Feng Liu)

which is local but with restriction on the objective function. In this paper, we consider the regulation of both active and reactive controllable power of DERs. In the controller design, partial primal-dual gradient algorithm is utilized, which is formulated as the form of the Krasnosel'skii-Mann iteration. In this way, the objective function is only required to be *convex* and have a Lipschitzian gradient, which relaxes the assumption commonly used in most of existing literature (*strong convexity* is required). Moreover, the operator splitting method is employed to convert the control algorithm into a fixed-point problem, which greatly simplifies the convergence proof. In terms of practical application, an online implementation method is provided to make the controller adjustable to time-varying environments.

The rest of this paper is organized as follows. In Section 2, we introduce some preliminaries and the model of distribution networks. Section 3 formulates the optimal voltage control problem. The asynchronous controller is investigated in Section 4. In Section 5, convergence and optimality of the equilibrium are proved. Section 6 introduces the implementation of the proposed method. We confirm the performance of controllers via simulations on an 8-bus system and IEEE 123-bus system in Section 7. Section 8 concludes the paper.

2. Preliminaries and System Modeling

2.1. Preliminaries

In this paper, \mathbb{R}^n (\mathbb{R}_+^n) is the n -dimensional (nonnegative) Euclidean space. For a column vector $x \in \mathbb{R}^n$ (matrix $A \in \mathbb{R}^{m \times n}$), x^T (A^T) denotes its transpose. For vectors $x, y \in \mathbb{R}^n$, $x^T y = \langle x, y \rangle$ denotes the inner product of x, y . $\|x\| = \sqrt{x^T x}$ denotes the norm induced by the inner product. For a positive definite matrix G , denote the inner product $\langle x, y \rangle_G = \langle Gx, y \rangle$. Similarly, the G -matrix induced norm $\|x\|_G = \sqrt{\langle Gx, x \rangle}$. Use I_n to denote the identity matrix with dimension n . Sometimes, we also omit n and use I to denote the identity matrix with proper dimension if there is no confusion. For a matrix $A = [a_{ij}]$, a_{ij} stands for the entry in the i -th row and j -th column of A . Use $\prod_{i=1}^n \Omega_i$ to denote the Cartesian product of the sets $\Omega_i, i = 1, \dots, n$. Given a collection of y_i for i in a certain set Y , define $\text{col}(y_j) := (y_1, y_2, \dots, y_n)^T$ and denote its vector form by $\mathbf{y} := \text{col}(y_j)$. Define the projection of x onto a set Ω as

$$\mathcal{P}_\Omega(x) = \arg \min_{y \in \Omega} \|x - y\| \quad (1)$$

Use Id to denote the identity operator, i.e., $\text{Id}(x) = x, \forall x$. Define the normal cone as $N_\Omega(x) = \{v | \langle v, y - x \rangle \leq 0, \forall y \in \Omega\}$. We have $\mathcal{P}_\Omega(x) = (\text{Id} + N_\Omega)^{-1}(x)$ Yi and Pavel (2019b), (Bauschke et al., 2011, Chapter 23.1).

For a set-valued operator $\mathcal{U} : \mathbb{R}^n \rightarrow 2^{\mathbb{R}^n}$, its domain is $\text{dom} \mathcal{U} := \{x \in \mathbb{R}^n | \mathcal{U}x \neq \emptyset\}$. The graph of \mathcal{U} is defined as $\text{gra} \mathcal{U} := \{(x, u) \in \mathbb{R}^n \times \mathbb{R}^n | u \in \mathcal{U}x\}$. An operator \mathcal{U} is monotone if $\forall (x, u), \forall (y, v) \in \text{gra} \mathcal{U}$, we have $\langle x - y, u - v \rangle \geq 0$. It is called maximally monotone if $\text{gra} \mathcal{U}$ is not strictly contained in the graph of any other monotone operator. For a single-valued operator $\mathcal{T} : \Omega \subset \mathbb{R}^n \rightarrow \mathbb{R}^n$, a point $x \in \Omega$ is a fixed point of \mathcal{T} if $\mathcal{T}(x) \equiv x$. The set

of fixed points of \mathcal{T} is denoted by $\text{Fix}(\mathcal{T})$. \mathcal{T} is nonexpansive if $\|\mathcal{T}(x) - \mathcal{T}(y)\| \leq \|x - y\|, \forall x, y \in \Omega$. \mathcal{T} is firmly nonexpansive if $\|\mathcal{T}(x) - \mathcal{T}(y)\|^2 + \|(\text{Id} - \mathcal{T})(x) - (\text{Id} - \mathcal{T})(y)\|^2 \leq \|x - y\|^2, \forall x, y \in \Omega$. For $\alpha \in (0, 1)$, \mathcal{T} is called α -averaged if there exists a nonexpansive operator \mathcal{S} such that $\mathcal{T} = (1 - \alpha)\text{Id} + \alpha\mathcal{S}$. We use $\mathcal{A}(\alpha)$ to denote the α -averaged operators. For $\beta \in \mathbb{R}_+^1$, \mathcal{T} is called β -cocoercive if $\beta\mathcal{T} \in \mathcal{A}(\frac{1}{2})$.

2.2. System Modeling

Consider a radial distribution network with $(n + 1)$ buses collected in the set $\mathcal{N}_0 := \{0\} \cup \mathcal{N}$, where $\mathcal{N} := \{1, \dots, n\}$ and bus 0 is the substation bus (slack bus) and is assumed to have a fixed voltage U_0 . Lines are denoted by the set $\mathcal{E} := \{(i, j)\} \subset \mathcal{N} \times \mathcal{N}$. Due to the tree topology, the cardinality of $|\mathcal{E}| = n$. Use N_j and N_j^2 to denote the neighbors and two-hop neighbors of bus j respectively.

For bus j , use U_j to denote its voltage magnitude. Use p_j and q_j to denote the active and reactive power generations respectively, which are controllable. p_j^c and q_j^c are active and reactive power loads, which are uncontrollable. For line $(i, j) \in \mathcal{E}$, use r_{ij} and x_{ij} to denote its line resistance and reactance. The active and reactive power from bus i to j is denoted by P_{ij} and Q_{ij} respectively. The linearized DistFlow equations are given as Baran and Wu (1989a,b); Zhu and Liu (2016)

$$P_{ij} + p_j - p_j^c = \sum_{k \in N_j} P_{jk} \quad (2a)$$

$$Q_{ij} + q_j - q_j^c = \sum_{k \in N_j} Q_{jk} \quad (2b)$$

$$U_i^2 - U_j^2 = r_{ij}P_{ij} + x_{ij}Q_{ij} \quad (2c)$$

The relative error of the linearization is very small, at the order of 1% Zhu and Liu (2016). Denote the incidence matrix of the network $(\mathcal{N}_0, \mathcal{E})$ by $\mathbf{M} \in \mathbb{R}^{(n+1) \times n}$. Moreover, use \mathbf{m}_0^T to denote the first row of \mathbf{M} , while the rest of the matrix is denoted by \mathbf{M} . Define $V_i := \frac{U_i^2}{2}$, and then the compact form of (2) is

$$\mathbf{M}\mathbf{P} = \mathbf{p} - \mathbf{p}^c \quad (3a)$$

$$\mathbf{M}\mathbf{Q} = \mathbf{q} - \mathbf{q}^c \quad (3b)$$

$$[\mathbf{m}_0, \mathbf{M}^T] \cdot [V_0, \mathbf{V}^T]^T = \text{diag}(\mathbf{r})\mathbf{P} + \text{diag}(\mathbf{x})\mathbf{Q} \quad (3c)$$

where $\text{diag}(\mathbf{r})$ is the diagonal matrix composed of r_{ij} , and similar is $\text{diag}(\mathbf{x})$. As the network is connected, the rank of \mathbf{M} is n . Thus, \mathbf{M} is of full rank and invertible Zhu and Liu (2016). Finally, we have

$$\mathbf{V} = \mathbf{R}\mathbf{p} + \mathbf{X}\mathbf{q} - \mathbf{M}^{-T}\mathbf{m}_0V_0 - \mathbf{R}\mathbf{p}^c - \mathbf{X}\mathbf{q}^c \quad (4)$$

where $\mathbf{R} = \mathbf{M}^{-T}\text{diag}(\mathbf{r})\mathbf{M}^{-1}$ and $\mathbf{X} = \mathbf{M}^{-T}\text{diag}(\mathbf{x})\mathbf{M}^{-1}$. \mathbf{R} and \mathbf{X} are all symmetric positive definite matrices. By Kekatos et al. (2015b, 2016), we know $-\mathbf{M}^{-T}\mathbf{m}_0 = \mathbf{1}_n$. Denote the inverse of \mathbf{X} by $\mathbf{B} = \mathbf{M}\text{diag}(\mathbf{x}^{-1})\mathbf{M}^T$, which is also positive definite. It is proved in (Zhou et al., 2018, Theorem 2) that $\mathbf{B} = \mathbf{L} + \text{diag}(\frac{1}{x_{0j}})$, where \mathbf{L} is the weighted Laplacian matrix of the subtree (i.e., without bus 0) and x_{0j} is the reactance of the line connected to bus 0. If bus j is not connected to the bus 0 directly, $x_{0j} = \infty$.

If the distribution network lines have unified resistance-reactance ratio, i.e. there exists a constant $K = \frac{r_{ij}}{x_{ij}}, \forall (i, j) \in \mathcal{E}$, the network is called homogeneous. For a homogeneous network, we have $\mathbf{R} = K\mathbf{X}$ and $\mathbf{B} \cdot \mathbf{R} = K$. In the analysis of

this paper, it is assumed that the distribution network is homogeneous, which is true in the most cases in practice Bolognani et al. (2015); Tang et al. (2019). In the simulation, however, we also use the heterogeneous network to verify the performance of the controller.

3. Problem Formulation

The optimal voltage control for a homogeneous network is formulated as

$$\min_{\mathbf{V}, \mathbf{p}, \mathbf{q}} f = \frac{1}{2} \|\mathbf{V} - \mathbf{V}^o\|^2 + \sum_{j \in \mathcal{N}} g_j(p_j, q_j) \quad (5a)$$

$$\text{s.t. } \mathbf{B}\mathbf{V} = \mathbf{K}\mathbf{p} + \mathbf{q} + \boldsymbol{\varpi}^s \quad (5b)$$

$$\underline{p}_j \leq p_j \leq \bar{p}_j, \forall j \quad (5c)$$

$$\underline{q}_j \leq q_j \leq \bar{q}_j, \forall j \quad (5d)$$

$$0 \leq p_j^2 + q_j^2 \leq s_j^2, \forall j \quad (5e)$$

where $\boldsymbol{\varpi}^s = \mathbf{B}(-\mathbf{M}^{-T}\mathbf{m}_0V_0 - \mathbf{R}\mathbf{p}^c - \mathbf{X}\mathbf{q}^c)$. \mathbf{V}^o is the desired voltage profile and set as $\mathbf{V}^o = 0.5 \times \mathbf{1}_n$. $\underline{p}_j, \bar{p}_j$ are lower and upper bounds of p_j . $\underline{q}_j, \bar{q}_j$ are lower and upper bounds of q_j . s_j is the apparent power capability of the inverter. The objective function is composed of two parts: voltage difference square, active and reactive power cost, for which we make an assumption.

Assumption 1. The function $g_i(x)$ is convex, and $\nabla g_i(x)$ is ϑ -Lipschitzian, i.e., for some $\vartheta > 0$, $\|\nabla g_i(x_1) - \nabla g_i(x_2)\| \leq \vartheta\|x_1 - x_2\|, \forall x_1, x_2$.

For each bus j , the feasible region is defined as

$$\Omega_j = \{ (p_j, q_j) \mid p_j, q_j \text{ satisfy (5c), (5d), (5e)} \}$$

The Lagrangian of (5) is

$$\mathcal{L}(\mathbf{V}, \mathbf{p}, \mathbf{q}, \boldsymbol{\lambda}) = \frac{1}{2} \|\mathbf{V} - \mathbf{V}^*\|^2 + \sum_{j \in \mathcal{N}} g_j(p_j, q_j) + \boldsymbol{\lambda}^T (\mathbf{B}\mathbf{V} - \mathbf{K}\mathbf{p} - \mathbf{q} - \boldsymbol{\varpi}^s) \quad (6)$$

where $\Omega = \prod_{j \in \mathcal{N}} \Omega_j$.

Remark 1 (Objective function). The item $g_j(p_j, q_j)$ in the objective function is more general compared with existing literature, which is only required to be convex and has a Lipschitzian gradient instead of strongly convex. If the objective function is formulated by a \mathbf{B} -induced norm, i.e., $f = \frac{1}{2} \|\mathbf{V} - \mathbf{V}^o\|_{\mathbf{B}}^2$, we can design a local controller, as done in Zhu and Liu (2016); Liu et al. (2017); Bolognani et al. (2015).

In the problem (5), we consider the regulation of both active and reactive power of DERs. The main motivations are two-folds: first, some DERs such as many small hydro plants have no capability of reactive power regulation; second, the distribution networks have comparable resistance and reactance. Thus, regulating both active and reactive power turns to be necessary in the voltage control of active distribution networks.

4. Asynchronous Voltage Control

In the asynchronous controller design, we adopt the partial primal-dual algorithm. Similar methods have been explored in

Li et al. (2016); Wang et al. (2019) for a continuous-time setting and Liu et al. (2018b) for the discrete setting. However, Liu et al. (2018b) does not design an asynchronous algorithm. In a partial primal-dual algorithm, \mathbf{V} is obtained by solving the following problem.

$$\mathbf{V}_t = \arg \min_{\mathbf{V}} \mathcal{L}(\mathbf{V}, \mathbf{p}_t, \mathbf{q}_t, \boldsymbol{\lambda}_t) = -\mathbf{B}^T \boldsymbol{\lambda}_t + \mathbf{V}^o \quad (7)$$

Define $\boldsymbol{\varpi}^a = \boldsymbol{\varpi}^s - \mathbf{B}\mathbf{V}^o$. Each bus has its own iteration number t_j , implying that a *local clock* is used. Then, various types of asynchrony can be considered as time intervals between two iterations. At t_j , bus j computes in the following way, which has the form of the Krasnosel'skii-Mann iteration.

$$\begin{bmatrix} \tilde{p}_{j,t_j} \\ \tilde{q}_{j,t_j} \end{bmatrix} = \mathcal{P}_{\Omega_j} \left[\begin{bmatrix} p_{j,t_j - \tau_j^j} \\ q_{j,t_j - \tau_j^j} \end{bmatrix} - \alpha_{pq} \begin{bmatrix} \frac{\partial g_j}{\partial p_j}(p_{j,t_j - \tau_j^j}, q_{j,t_j - \tau_j^j}) - K \lambda_{j,t_j - \tau_j^j} \\ \frac{\partial g_j}{\partial q_j}(p_{j,t_j - \tau_j^j}, q_{j,t_j - \tau_j^j}) - \lambda_{j,t_j - \tau_j^j} \end{bmatrix} \right] \quad (8a)$$

$$\tilde{\lambda}_{j,t_j} = \lambda_{j,t_j - \tau_j^j} + \alpha_\lambda \left(- \sum_{k \in N_j \cup N_j^2} \tilde{B}_{jk} \lambda_{k,t_k - \tau_k^k} - 2K \tilde{p}_{j,t_j} - 2\tilde{q}_{j,t_j} + K p_{j,t_j - \tau_j^j} + q_{j,t_j - \tau_j^j} - \boldsymbol{\varpi}_j^a \right) \quad (8b)$$

$$\lambda_{j,t_j+1} = \lambda_{j,t_j - \tau_j^j} + \eta (\tilde{\lambda}_{j,t_j} - \lambda_{j,t_j - \tau_j^j}) \quad (8c)$$

$$p_{j,t_j+1} = p_{j,t_j - \tau_j^j} + \eta (\tilde{p}_{j,t_j} - p_{j,t_j - \tau_j^j}) \quad (8d)$$

$$q_{j,t_j+1} = q_{j,t_j - \tau_j^j} + \eta (\tilde{q}_{j,t_j} - q_{j,t_j - \tau_j^j}) \quad (8e)$$

$$V_{j,t_j+1} = - \sum_{k \in N_j} B_{jk} \lambda_{j,t_j+1} + V_j^o \quad (8f)$$

where $\boldsymbol{\varpi}_j^a$ is the j -th component of $\boldsymbol{\varpi}^a$ and stepsizes $\eta, \alpha_{pq}, \alpha_\lambda > 0$. \tilde{B}_{jk} is the j th row and k th column element of matrix $\tilde{\mathbf{B}} = \mathbf{B}^2$. As \mathbf{B} has the same sparse structure with Laplacian of the subtree, the matrix \mathbf{B}^2 has nonzero entries matching the neighbors and two-hop neighbors of each bus. This implies that each bus only needs the information of its neighbors and two-hop neighbors to compute the variable $\tilde{\lambda}_{j,t_j}$. The asynchronous distributed voltage control (ASDVC) algorithm based on (8) is given in Algorithm 1.

Algorithm 1 ASDVC

Input: For bus j , the input is $(p_{j,0}, q_{j,0}) \in \Omega_j, \lambda_{j,0} \in \mathbb{R}$.

Iteration at t_j : Suppose bus j 's clock ticks at time t_j , then bus j is activated and updates its local variables as follows:

Step 1: Reading phase

Get $\lambda_{k,t_k - \tau_k^k}, k \in N_j \cup N_j^2$ from its neighbors' and two-hop neighbors' output cache.

Step 2: Computing phase

Calculate $\tilde{p}_{j,t_j}, \tilde{q}_{j,t_j}$ and $\tilde{\lambda}_{j,t_j}$ according to (8a) and (8b) respectively.

Update $\lambda_{j,t_j+1}, p_{j,t_j+1}, q_{j,t_j+1}$ and V_{j,t_j+1} according to (8c) – (8f) respectively.

Step 3: Writing phase

Write λ_{j,t_j+1} to its output cache and $p_{j,t_j+1}, q_{j,t_j+1}, V_{j,t_j+1}$ to its local storage. Increase t_j to $t_j + 1$.

Remark 2 (Asynchronous update). The main difference between this paper and Liu et al. (2018b) is that we design the asynchronous pattern for the partial primal-dual algorithm. It should be noted that this is not trivial. As proved in Hale et al. (2017), the asynchronous distributed primal-dual algorithm cannot guarantee the convergence if dual variables are not updated simultaneously. In ASDVC, there is no need to update λ simultaneously. To this end, we use neighbors' and two-hop neighbors' information.

5. Optimality and Convergence

In this section, we formulate the algorithm (8) into a fixed-point iteration problem using operator-splitting method. Then, its convergence and optimality of the equilibrium are proved.

5.1. Algorithm Reformulation

Define $z_j = \text{col}(p_j, q_j)$, $\tilde{z}_j = \text{col}(\tilde{p}_j, \tilde{q}_j)$. If the time delay is not considered, the compact form of (8) can be obtained, denoted by SDVC. As \mathbf{V} is not in the iteration process, we omit it here.

$$\tilde{\mathbf{z}}_t = \mathcal{P}_\Omega(\mathbf{z}_t - \alpha_{pq}(\nabla_{z_t} g(z_t) - \text{col}(K\lambda_t, \lambda_t))) \quad (9a)$$

$$\tilde{\lambda}_t = \lambda_t + \alpha_\lambda(-\mathbf{B}^2\lambda_t - 2(K \cdot I_n, I_n)\tilde{\mathbf{z}}_t + (K \cdot I_n, I_n)\mathbf{z}_t - \varpi^a) \quad (9b)$$

$$\mathbf{z}_{t+1} = \mathbf{z}_t + \eta(\tilde{\mathbf{z}}_t - \mathbf{z}_t) \quad (9c)$$

$$\lambda_{t+1} = \lambda_t + \eta(\tilde{\lambda}_t - \lambda_t) \quad (9d)$$

In the rest of the paper, denote $F(\mathbf{z}) = \nabla_{z_t} g(\mathbf{z})$. Equations (9a)-(9b) are equivalent to ¹

$$-F(\mathbf{z}_t) = N_\Omega(\tilde{\mathbf{z}}_t) - \text{col}(K\tilde{\lambda}_t, \tilde{\lambda}_t) + \alpha_{pq}^{-1}(\tilde{\mathbf{z}}_t - \mathbf{z}_t) + (K \cdot I_n, I_n)^T(\tilde{\lambda}_t - \lambda_t) \quad (10a)$$

$$-\varpi^a - \mathbf{B}^2\lambda_t = (K \cdot I_n, I_n)\tilde{\mathbf{z}}_t + (K \cdot I_n, I_n)(\tilde{\mathbf{z}}_t - \mathbf{z}_t) + \alpha_\lambda^{-1}(\tilde{\lambda}_t - \lambda_t) \quad (10b)$$

Define following two operators

$$\mathcal{C} : \begin{bmatrix} \mathbf{z} \\ \lambda \end{bmatrix} \mapsto \begin{bmatrix} F(\mathbf{z}) \\ \varpi^a + \mathbf{B}^2\lambda \end{bmatrix} \quad (11a)$$

$$\mathcal{D} : \begin{bmatrix} \mathbf{z} \\ \lambda \end{bmatrix} \mapsto \begin{bmatrix} N_\Omega(\mathbf{z}) - \text{col}(K\lambda, \lambda) \\ (K \cdot I_n, I_n)\mathbf{z} \end{bmatrix} \quad (11b)$$

and denote $\mathbf{w}_t = \text{col}(\mathbf{z}_t, \lambda_t)$ and $\tilde{\mathbf{w}}_t = \text{col}(\tilde{\mathbf{z}}_t, \tilde{\lambda}_t)$.

Then, (10) can be rewritten as

$$-\mathcal{C}(\mathbf{w}_t) = \mathcal{D}(\tilde{\mathbf{w}}_t) + \Gamma \cdot (\tilde{\mathbf{w}}_t - \mathbf{w}_t) \quad (12)$$

where

$$\Gamma := \begin{bmatrix} \alpha_{pq}^{-1}I_{2n} & (K \cdot I_n, I_n)^T \\ (K \cdot I_n, I_n) & \alpha_\lambda^{-1}I_n \end{bmatrix} \quad (13)$$

Here, $\alpha_{pq}, \alpha_\lambda$ are chosen to make Γ is positive definite.

Denote the maximal and minimal eigenvalues of \mathbf{B} by σ_{\max} and σ_{\min} respectively. We have the following result.

Lemma 1. In terms of \mathcal{C} and \mathcal{D} , we have following properties.

- 1) Operator \mathcal{C} is β -cocoercive under the 2-norm with $0 < \beta \leq \min\{\frac{1}{\sigma_{\max}^2}, \frac{1}{\beta}\}$;
- 2) Operator \mathcal{D} is maximally monotone;
- 3) $\Gamma^{-1}\mathcal{D}$ is maximally monotone under the Γ -induced norm $\|\cdot\|_\Gamma$;
- 4) $(\text{Id} + \Gamma^{-1}\mathcal{D})^{-1}$ exists and is firmly nonexpansive.

Proof. 1): According to the definition of \mathcal{C} and the definition of β -cocoercive, it suffice to prove that $\langle \mathcal{C}(\mathbf{w}_1) - \mathcal{C}(\mathbf{w}_2), \mathbf{w}_1 - \mathbf{w}_2 \rangle \geq \beta \|\mathcal{C}(\mathbf{w}_1) - \mathcal{C}(\mathbf{w}_2)\|^2$, or equivalently

$$(F(\mathbf{z}_1) - F(\mathbf{z}_2))^T(\mathbf{z}_1 - \mathbf{z}_2) + (\lambda_1 - \lambda_2)^T \mathbf{B}^2(\lambda_1 - \lambda_2) \geq \beta(\|\mathbf{B}^2\lambda_1 - \mathbf{B}^2\lambda_2\|^2 + \|F(\mathbf{z}_1) - F(\mathbf{z}_2)\|^2) \quad (14)$$

Notice that $\varpi^a + \mathbf{B}^2\lambda$ is the gradient of function $\hat{f}(\lambda) = \frac{1}{2}\lambda^T \mathbf{B}^2\lambda + \lambda^T \varpi^a$. As $\nabla^2 \hat{f}(\lambda) = \mathbf{B}^2 > 0$, $\hat{f}(\lambda)$ is a convex function. For its gradient, we have

$$\|\mathbf{B}^2(\lambda_1 - \lambda_2)\| \leq \|\mathbf{B}^2\| \|\lambda_1 - \lambda_2\| = \sigma_{\max}^2 \|\lambda_1 - \lambda_2\| \quad (15)$$

Thus, $\nabla \hat{f}(\lambda)$ is σ_{\max}^2 -Lipschitzian. Then, $\nabla \hat{f}(\lambda) = \varpi^a + \mathbf{B}^2\lambda$ is $\frac{1}{\sigma_{\max}^2}$ -cocoercive (Bauschke et al., 2011, Corollary 18.16), i.e.,

$$(\lambda_1 - \lambda_2)^T \mathbf{B}^2(\lambda_1 - \lambda_2) \geq \frac{1}{\sigma_{\max}^2} \|\mathbf{B}^2\lambda_1 - \mathbf{B}^2\lambda_2\|^2 \quad (16)$$

Moreover, since F is $\frac{1}{\beta}$ -cocoercive, i.e.,

$$(F(\mathbf{z}_1) - F(\mathbf{z}_2))^T(\mathbf{z}_1 - \mathbf{z}_2) \geq \frac{1}{\beta} \|F(\mathbf{z}_1) - F(\mathbf{z}_2)\|^2 \quad (17)$$

Combining (16), (17) and taking $0 < \beta \leq \min\{\frac{1}{\sigma_{\max}^2}, \frac{1}{\beta}\}$, we can get the first assertion.

2): The operator \mathcal{D} can be rewritten as

$$\mathcal{D} = \begin{bmatrix} 0 & -(KI_n, I_n)^T \\ (KI_n, I_n) & 0 \end{bmatrix} \begin{bmatrix} \mathbf{z} \\ \lambda \end{bmatrix} + \begin{bmatrix} N_\Omega(\mathbf{z}) \\ 0 \end{bmatrix} = \mathcal{D}_1 + \mathcal{D}_2 \quad (18)$$

As \mathcal{D}_1 is a skew-symmetric matrix, \mathcal{D}_1 is maximally monotone (Bauschke et al., 2011, Example 20.30). Moreover, $N_\Omega(\mathbf{z})$ and 0 are all maximally monotone (Bauschke et al., 2011, Example 20.41), so \mathcal{D}_2 is also maximally monotone. Thus, $\mathcal{D} = \mathcal{D}_1 + \mathcal{D}_2$ is maximally monotone.

3) As Γ is symmetric positive definite and \mathcal{D} is maximally monotone, we can prove that $\Gamma^{-1}\mathcal{D}$ is maximally monotone by the similar analysis in Lemma 5.6 of Yi and Pavel (2019b).

4) As $\Gamma^{-1}\mathcal{D}$ is maximally monotone, $(\text{Id} + \Gamma^{-1}\mathcal{D})^{-1}$ exists and is firmly nonexpansive by (Bauschke et al., 2011, Proposition 23.7). \square

By the last assertion of Lemma 1, (9) is equivalent to

$$\tilde{\mathbf{w}}_t = (\text{Id} + \Gamma^{-1}\mathcal{D})^{-1}(\text{Id} - \Gamma^{-1}\mathcal{C})\mathbf{w}_t \quad (19a)$$

$$\mathbf{w}_{t+1} = \mathbf{w}_t + \eta(\tilde{\mathbf{w}}_t - \mathbf{w}_t) \quad (19b)$$

Denote $\mathcal{S}_1 = (\text{Id} + \Gamma^{-1}\mathcal{D})^{-1}$, $\mathcal{S}_2 = (\text{Id} - \Gamma^{-1}\mathcal{C})$ and $\mathcal{S} = \mathcal{S}_1\mathcal{S}_2$, and then we have following results.

Lemma 2. Take $0 < \beta \leq \min\{\frac{1}{\sigma_{\max}^2}, \frac{1}{\beta}\}$, $\kappa > \frac{1}{2\beta}$, and the step sizes $\alpha_{pq}, \alpha_\lambda$ such that $\Gamma - \kappa I$ is positive semi-definite. Following results are true under the Γ -induced norm $\|\cdot\|_\Gamma$.

¹The “=” in (10a) is substituted by “ \leq ” in some literature. Here, we still use “=” for the notation consistence if there is no confusion.

- 1) \mathcal{S}_1 is a $\frac{1}{2}$ -averaged operator, i.e., $\mathcal{S}_1 \in \mathcal{A}(\frac{1}{2})$;
- 2) \mathcal{S}_2 is a $\frac{1}{2\beta\kappa}$ -averaged operator, i.e., $\mathcal{S}_2 \in \mathcal{A}(\frac{1}{2\beta\kappa})$;
- 3) \mathcal{S} is a $\frac{2\kappa\beta}{4\kappa\beta-1}$ -averaged operator, i.e., $\mathcal{S} \in \mathcal{A}(\frac{2\kappa\beta}{4\kappa\beta-1})$.

Proof. 1): From the assertion 4) of Lemma 1, $\mathcal{S}_1 = (\text{Id} + \Gamma^{-1}\mathcal{D})^{-1}$ is firmly nonexpansive, implying $\mathcal{S}_1 \in \mathcal{A}(\frac{1}{2})$.

2): First, we prove that $\Gamma^{-1}C$ is $\beta\kappa$ -cocoercive, i.e.,

$$\begin{aligned} \langle \Gamma^{-1}C(\mathbf{w}_1) - \Gamma^{-1}C(\mathbf{w}_2), \mathbf{w}_1 - \mathbf{w}_2 \rangle_{\Gamma} &\geq \\ \beta\kappa \|\Gamma^{-1}C(\mathbf{w}_1) - \Gamma^{-1}C(\mathbf{w}_2)\|_{\Gamma}^2 & \end{aligned} \quad (20)$$

Denote the maximal and minimal eigenvalues of Γ by δ_{\max} and δ_{\min} respectively, and we have $\delta_{\max} \geq \delta_{\min} \geq \kappa > 0$. Moreover, the Euclidean norms of Γ and Γ^{-1} are $\|\Gamma\|_2 = \delta_{\max}$ and $\|\Gamma^{-1}\|_2 = \frac{1}{\delta_{\min}}$ (Meyer, 2000, Proposition 5.2.7, 5.2.8).

For the right hand side of (20), we have

$$\begin{aligned} \beta\kappa \|\Gamma^{-1}C(\mathbf{w}_1) - \Gamma^{-1}C(\mathbf{w}_2)\|_{\Gamma}^2 &= \beta\kappa \|C(\mathbf{w}_1) - C(\mathbf{w}_2)\|_{\Gamma^{-1}}^2 \\ &= \beta\kappa (C(\mathbf{w}_1) - C(\mathbf{w}_2))^T \Gamma^{-1} (C(\mathbf{w}_1) - C(\mathbf{w}_2)) \\ &\leq \beta\kappa \|\Gamma^{-1}\|_2 \|C(\mathbf{w}_1) - C(\mathbf{w}_2)\|_2^2 \\ &\leq \beta\kappa \cdot \frac{1}{\kappa} \|C(\mathbf{w}_1) - C(\mathbf{w}_2)\|_2^2 \end{aligned} \quad (21)$$

where the first " \leq " is due to the Cauchy-Schwarz inequality and the second is due to $\delta_{\min} \geq \kappa$.

For the left part of (20), we have

$$\begin{aligned} \langle \Gamma^{-1}C(\mathbf{w}_1) - \Gamma^{-1}C(\mathbf{w}_2), \mathbf{w}_1 - \mathbf{w}_2 \rangle_{\Gamma} &= \langle C(\mathbf{w}_1) - C(\mathbf{w}_2), \mathbf{w}_1 - \mathbf{w}_2 \rangle \\ &\geq \beta \|C(\mathbf{w}_1) - C(\mathbf{w}_2)\|_2^2 \end{aligned} \quad (22)$$

where the inequality is from assertion 1) of Lemma 1. From (21) and (22), we have (20).

As $\Gamma^{-1}C$ is $\beta\kappa$ -cocoercive, we have $\beta\kappa\Gamma^{-1}C \in \mathcal{A}(\frac{1}{2})$. That is to say, there is a nonexpansive operator $\tilde{\mathcal{S}}$ such that $\beta\kappa\Gamma^{-1}C = \frac{1}{2}\text{Id} + \frac{1}{2}\tilde{\mathcal{S}}$, i.e., $\Gamma^{-1}C = \frac{1}{2\beta\kappa}\text{Id} + \frac{1}{2\beta\kappa}\tilde{\mathcal{S}}$. Then,

$$\mathcal{S}_2 = \text{Id} - \Gamma^{-1}C = \left(1 - \frac{1}{2\beta\kappa}\right)\text{Id} - \frac{1}{2\beta\kappa}\tilde{\mathcal{S}} \quad (23)$$

As $0 < \frac{1}{2\beta\kappa} < 1$ and $-\tilde{\mathcal{S}}$ is also nonexpansive, we have $\mathcal{S}_2 \in \mathcal{A}(\frac{1}{2\beta\kappa})$.

3): From (Combettes and Yamada, 2015, Proposition 2.4), $\mathcal{S} = \mathcal{S}_1\mathcal{S}_2$ is a a -averaged operator with $a = \frac{a_1+a_2-2a_1a_2}{1-a_1a_2}$, if \mathcal{S}_1 is a_1 -averaged and \mathcal{S}_2 is a_2 -averaged. As $\mathcal{S}_1 \in \mathcal{A}(\frac{1}{2\beta\kappa})$ and $\mathcal{S}_2 \in \mathcal{A}(\frac{1}{2})$, we have $\mathcal{S} \in \mathcal{A}(\frac{2\kappa\beta}{4\kappa\beta-1})$. \square

By the definition of the averaged operator and assertion 3) of Lemma 2, there exists a nonexpansive operator \mathcal{T} such that

$$\mathcal{S} = \left(1 - \frac{2\kappa\beta}{4\kappa\beta-1}\right)\text{Id} + \frac{2\kappa\beta}{4\kappa\beta-1}\mathcal{T} \quad (24)$$

Apparently, operators \mathcal{S} and \mathcal{T} have the same fixed points, i.e., $\text{Fix}(\mathcal{S}) = \text{Fix}(\mathcal{T})$.

We convert the asynchronous algorithm into a fixed-point iteration problem with an averaged operator. Moreover, we also construct a nonexpansive operator \mathcal{T} , which enables us to prove the convergence of the asynchronous algorithm ASDVC.

5.2. Optimality of the equilibrium point

The definition of the equilibrium point of ASDVC is introduced as follows.

Definition 1. A point $\mathbf{w}^* = \text{col}(w_j^*) = \text{col}(x_j^*, \lambda_j^*)$ is an equilibrium point of system (8) if $\lim_{t_j \rightarrow \infty} w_{t_j} = w_j^*, \forall j$ holds.

Now, we give the KKT condition of the optimization problem (5) (Ruszczynski and Ruszczynski, 2006, Theorem 3.25).

$$0 = (\mathbf{V} - \mathbf{V}^o) + \mathbf{B}^T \lambda \quad (25a)$$

$$0 = \nabla_{\mathbf{z}} g(\mathbf{z}) - \text{col}(K\lambda, \lambda) + N_{\Omega}(\mathbf{z}) \quad (25b)$$

$$0 = \boldsymbol{\varpi}^s - \mathbf{B}\mathbf{V} + (K \cdot I, I)\mathbf{z} \quad (25c)$$

Denote $\mathbf{V}^* = -\mathbf{B}^T \lambda^* + \mathbf{V}^o$, and we have the following result.

Theorem 3. The point $(\mathbf{V}^*, \mathbf{z}^*, \lambda^*)$ satisfies the KKT condition (25), i.e., it is the primal-dual optimal solution to the optimization problem (5).

Proof. By Definition 1, we know $w_j^* = \lim_{t_j \rightarrow \infty} w_{j,t_j-1} = \lim_{t_j \rightarrow \infty} w_{j,t_j} = \lim_{t_j \rightarrow \infty} w_{j,t_j+1} = \lim_{t_j \rightarrow \infty} \tilde{w}_{j,t_j}$. From (10), we have

$$-(\mathbf{V}^* - \mathbf{V}^o) = \mathbf{B}^T \lambda^* \quad (26a)$$

$$-\nabla_{\mathbf{z}^*} g(\mathbf{z}^*) = N_{\Omega}(\mathbf{z}^*) - \text{col}(K\lambda^*, \lambda^*) \quad (26b)$$

$$-\boldsymbol{\varpi}^s = -\mathbf{B}\mathbf{V}^* + (K \cdot I, I)\mathbf{z}^* \quad (26c)$$

Comparing (25) and (26), we know $(\mathbf{V}^*, \mathbf{z}^*, \lambda^*)$ satisfies the KKT condition. This completes the proof. \square

5.3. Convergence analysis

In this subsection, we investigate the convergence of ASDVC. We first treat ASDVC as a randomized block-coordinate fixed-point iteration problem with delayed information. Then, the results in Peng et al. (2016) can be applied.

To prove the convergence of ASDVC, we need introduce a global clock to substitute the local clocks of individual buses in ASDVC. The main idea is to queue t_j of all buses in the order of real time, and use a new number t to denote the t -th iteration in the queue. Take two local clocks as an example. Suppose the local clocks to be $t_1 = \{1, 3, 5, \dots\}$ and $t_2 = \{2, 4, 6, \dots\}$, and then the global clock is $t = \{1, 2, 3, 4, 5, 6, \dots\}$. In the global clock, it is assumed that the probability bus j is activated to update its local variables follows a uniform distribution. Hence, each bus is activated with the same probability. Note that the global clock is only used for convergence analysis, but it does not exist in the application.

Define vectors $\psi_j \in \mathbb{R}^{3n}, j \in \mathcal{N}$. The i th entry of ψ_j is denoted by $[\psi_j]_i$. Define $[\psi_j]_i = 1$ if the i th coordinate of \mathbf{w} is also a coordinate of w_j , and $[\psi_j]_i = 0$, otherwise. Denote by ξ a random variable (vector) taking values in $\psi_j, j \in \mathcal{N}$. Then $\text{Prob}(\xi = \psi_j) = 1/n$ also follows a uniform distribution. Let ξ_t be the value of ξ at the t th iteration. Then, a randomized block-coordinate fixed-point iteration for (19) is given by

$$\mathbf{w}_{t+1} = \mathbf{w}_t + \eta \xi_t \circ (\mathcal{S}(\mathbf{w}_t) - \mathbf{w}_t) \quad (27)$$

where \circ denotes the Hadamard product. In (27), only one bus j is activated at each iteration.

Since (27) is delay-free, we further modify it for considering delayed information, which is

$$\mathbf{w}_{t+1} = \mathbf{w}_t + \eta \xi_t \circ (\mathcal{S}(\hat{\mathbf{w}}_t) - \mathbf{w}_t) \quad (28)$$

where $\hat{\mathbf{w}}_t$ is the information with delay at iteration t . We will show that Algorithm 1 can be written as (28) if $\hat{\mathbf{w}}_t$ is properly defined. Suppose bus j is activated at the iteration t , then $\hat{\mathbf{w}}_t$ is defined as follows. For bus j , replace p_{j,t_j} , q_{j,t_j} and λ_{j,t_j} with $p_{j,t_j-\tau_j^j}$, $q_{j,t_j-\tau_j^j}$ and $\lambda_{j,t_j-\tau_j^j}$. Similarly, replace λ_{k,t_k} with $\lambda_{k,t_k-\tau_k^k}$ from its neighbors and two-hop neighbors. For inactivated buses, their state values keep unchanged.

Before proving the convergence, we make an assumption.

Assumption 2. The maximal time delay between two consecutive iterations is bounded by χ , i.e., $\{\max\{\tau_j^j\}\} \leq \chi, \forall t, \forall j$.

With the assumption, we have the convergence result.

Theorem 4. Suppose Assumptions 1, 2 holds. Take $0 < \beta \leq \min\{\frac{1}{\sigma_{\max}}, \frac{1}{\theta}\}$, $\kappa > \frac{1}{2\beta}$, and the step sizes $\alpha_{pq}, \alpha_\lambda$ such that $\Gamma - \kappa I$ is positive semi-definite. Choose $0 < \eta < \frac{1}{1+2\chi/\sqrt{n}} \frac{4\kappa\beta-1}{2\kappa\beta}$. Then, with ASDVC, \mathbf{w}_t converges to the point \mathbf{w}^* defined in Definition 1 with probability 1.

Proof. Combining (24) and (28), we have

$$\begin{aligned} \mathbf{w}_{t+1} &= \mathbf{w}_t + \eta \xi_t \circ \left(\left(1 - \frac{2\kappa\beta}{4\kappa\beta-1}\right) \hat{\mathbf{w}}_t - \mathbf{w}_t + \frac{2\kappa\beta}{4\kappa\beta-1} \mathcal{T}(\hat{\mathbf{w}}_t) \right) \\ &= \mathbf{w}_t + \eta \xi_t \circ \left(\hat{\mathbf{w}}_t - \mathbf{w}_t + \frac{2\kappa\beta}{4\kappa\beta-1} (\mathcal{T}(\hat{\mathbf{w}}_t) - \hat{\mathbf{w}}_t) \right) \end{aligned} \quad (29)$$

With $w_{j,t-\tau_j^j} = w_{j,t-\tau_j^j+1} = \dots = w_{j,t}$, we have $\xi_t \circ (\hat{\mathbf{w}}_t - \mathbf{w}_t) = 0$. Thus, (29) is equivalent to

$$\mathbf{w}_{t+1} = \mathbf{w}_t + \frac{2\eta\kappa\beta}{4\kappa\beta-1} \xi_t \circ (\mathcal{T}(\hat{\mathbf{w}}_t) - \hat{\mathbf{w}}_t) \quad (30)$$

In fact, (30) has the form of the ARock algorithms proposed in Peng et al. (2016). In Lemma 13 and Theorem 14 of Peng et al. (2016), it is proved that \mathbf{w}_t generated by (30) is bounded. Moreover, if η satisfies $0 < \eta < \frac{1}{1+2\chi/\sqrt{n}} \frac{4\kappa\beta-1}{2\kappa\beta}$, \mathbf{w}_t converges to a random variable that takes value in the fixed points of \mathcal{T} with probability 1, denoted by \mathbf{w}^* . Recall $Fix(\mathcal{S}) = Fix(\mathcal{T})$ and Theorem 3, and we know that \mathbf{w}^* satisfies the KKT condition (25), i.e., the equilibrium in Definition 1. This completes the proof. \square

Remark 3 (Nonexpansive operator). As \mathcal{S} is $\frac{2\kappa\beta}{4\kappa\beta-1}$ -averaged, it is also a nonexpansive operator (Bauschke et al., 2011, Remark 4.24). Then, in Theorem 4, we can also use \mathcal{S} instead of \mathcal{T} to prove the convergence of ASDVC. In this situation, the bound of η is $0 < \eta < \frac{1}{1+2\chi/\sqrt{n}}$. Since $\kappa > \frac{1}{2\beta}$, we have $\frac{4\kappa\beta-1}{2\kappa\beta} > 1$. This implies that the operator \mathcal{T} can increase the upper bound of η compared with \mathcal{S} .

6. Implementation

6.1. Communication graph

Although two-hop neighbors' information is utilized in the algorithm (8), the communication graph still can be fully distributed, i.e., neighboring communication. In (8b), two-hop

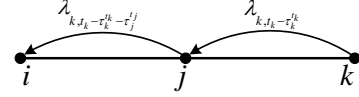


Figure 1: Two-step communications

neighbors' information is needed to obtain \tilde{B}_{jk} and $\lambda_{k,t_k-\tau_k^k}, k \in N_j^2$. For \tilde{B}_{jk} , it can be obtained from twice neighboring communications. In addition, as the topology of a distribution network does not change frequently, \tilde{B}_{jk} can be obtained in advance. For $\lambda_{k,t_k-\tau_k^k}, k \in N_j^2$, it also can be obtained from neighboring communications, which is illustrated in Fig.1.

Node i can get the information of node k by twice communications. In this situation, the time delay may be longer. As this is the asynchronous algorithm, we treat $\tau_j^j + \tau_k^k$ as one delay τ_k^k if there is no confusion. Then, one step and two-step communication delays can be formulated into a uniform framework. In this way, only neighboring communications are needed in the asynchronous algorithm.

6.2. Online Implementation

In the ASDVC, ϖ_j^a is assumed to be available for every bus j . By its definition, ϖ_j^a is determined by almost all of the power injection in the network, which implies that a centralized method is needed to get their values. Thus, if the system states vary rapidly with the variation of renewable generations and loads, they are difficult to obtain. From (5b), ϖ^s can be obtained from an equivalent way if we can measure the local voltage, active and reactive power injections and get the neighbors' voltages. Similar is ϖ^a due to $\varpi^a = \varpi^s - \mathbf{B}\mathbf{V}^o$. Denote the set of buses connected directly to bus 0 by N_0 . If we set $\mathbf{V}^o = 0.5 \times \mathbf{1}$, we have $\mathbf{B}\mathbf{V}^o = \begin{cases} 0, & j \notin N_0 \\ \frac{1}{2x_{0j}}, & j \in N_0 \end{cases}$. Then, ϖ_j^a in the ASDVC algorithm can be obtained by

$$\varpi_j^a = \begin{cases} -\sum_{k \in N_j} B_{jk} V_k^m + K p_j^m + q_j^m, & j \notin N_0 \\ -\frac{1}{2x_{0j}} - \sum_{k \in N_j} B_{jk} V_k^m + K p_j^m + q_j^m, & j \in N_0 \end{cases} \quad (31)$$

where p_j^m, q_j^m are measured active and reactive power locally and V_k^m is the square of measured voltage of the neighbor.

In (31), only communications between neighbors are needed. We can also use $p_{j,t}, q_{j,t}$ instead of p_j^m, q_j^m to avoid power measurements. In the inverter integrated DERs, $p_{j,t} \approx p_j^m$ and $q_{j,t} \approx q_j^m$ as the response is very fast. The voltage measurements contain the latest system information, which makes the implementation track the time-varying operating conditions.

7. Case Studies

In this section, simulation results are presented to demonstrate the effectiveness of the proposed voltage control methods. To this end, an 8-bus feeder and the IEEE 123-bus feeder are utilized as test systems. Each bus is equipped with a certain amount of PVs, which are able to offer flexible active and reactive power supplies to the feeder. Some buses have other controllable DERs like small hydro plants and energy storage systems. The simulations are implemented in Matlab R2017b simulator, and the OpenDSS is used for solving the ac power flow.

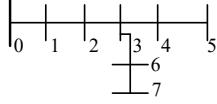


Figure 2: The graph of the 8-bus distribution network

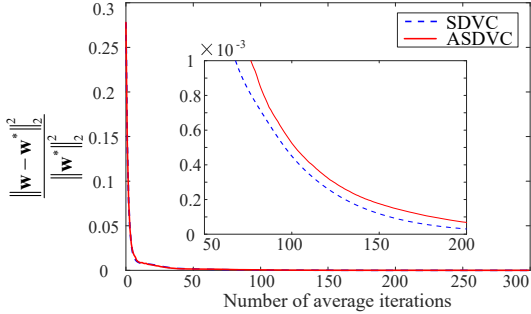


Figure 3: Comparison of algorithm convergence in terms of number of average iterations for SDVC and ASDVC. In the ASDVC, the random delay between 0 ~ 10 iterations is considered.

7.1. 8-bus feeder

An 8-bus distribution network is considered Tang et al. (2019), whose diagram is shown in Fig.2. The impedance of each line segment is identical, which is $0.9216 + j0.4608 \Omega$ with $K = 2$. All buses except bus 0 are equipped with DERs with active power limit as $\bar{\mathbf{p}} = -\underline{\mathbf{p}} = [90, 100, 0, 120, 170, 90, 70]\text{kW}$, reactive power limit as $\bar{\mathbf{q}} = -\underline{\mathbf{q}} = [100, 100, 110, 100, 130, 100, 120]\text{kVar}$. The capacity limit of inverter at each bus is $0.9 * \sqrt{\bar{\mathbf{p}}^2 + \bar{\mathbf{q}}^2}\text{kVA}$.

We first use CPLEX to obtain the optimal solution, which is $\mathbf{V}^* = [0.9934, 1.0063, 1.0083, 1.0282, 0.9492, 1.0073, 0.9987]$, $\mathbf{p}^* = [63.08, 65.41, 0, 120, 170, 70.57, 70]\text{kW}$, $\mathbf{q}^* = [31.53, 32.71, 63, 73.24, 90.54, 35.28, 41.29]\text{kVar}$. Then, SDVC and ASDVC are utilized in the voltage control in 8-bus feeder. We compare the controllers' performance by showing how $\frac{\|w-w^*\|_2^2}{\|w^*\|_2^2}$ is evolving with the number of average iterations of each MG, which is given in Fig.3. The SDVC and ASDVC algorithms have similar convergence speed, taking about 50 iterations. In contrast, ASDVC is only a bit of inferior to SDVC in terms of the number of average iterations.

7.2. IEEE 123-bus feeder

In addition to the 8-bus feeder, we also test the proposed method on the IEEE 123-bus system to show the scalability and practicability, the diagram of which is shown in Fig.4. It should be noted that the IEEE 123-bus system is not homogeneous, where the r_{ij}/x_{ij} ranges from 0.42 ~ 2.02. In the simulation, we take $K = 1$, which also shows the robustness of our method. In this case, the real data of residential load and solar generation is utilized. The minute-sampled profiles of active and reactive load are from an online data repository UCI (2012), and we use the data of July 13th, 2010. The minute-sampled profile of solar generation is from NREL (2018), which were collected in a city in Utah, U.S. and we use the data of July 14th, 2010. The profiles of active, reactive loads and solar generation are given in Fig.5, where the black curve is the active power (kW), red curve is the reactive power (kVar) and dotted blue line is the solar generation (kW). In the simulation, the tap positions of voltage

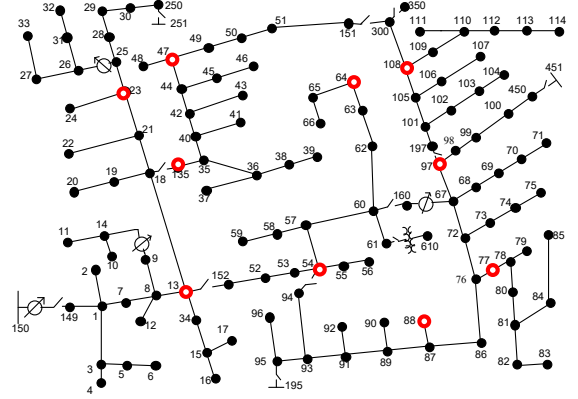


Figure 4: IEEE 123-bus system

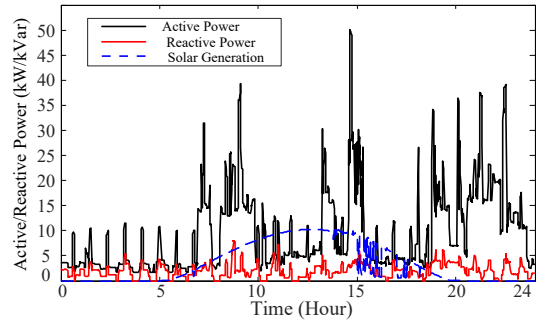


Figure 5: Active, reactive loads and solar generation within 24 hours

regulators are held constant in order to better capture the performance of proposed method. The voltage at the substation of the feeder head is set as 1 p.u. and the value of \mathbf{V}^0 is $0.5 \times \mathbf{1}$ p.u.. Each residential home is equipped with a solar generation. The capacity limit at each bus is 20kVA. The upper limit of active power is the instantaneous generation of the PV and the reactive power limit is determined correspondingly. Some buses are equipped with small hydro plants (marked as red in Fig.4). The active power limits are 300kW. When load and solar generation change, the method in Section 6.2 is utilized for the online implementation. In each minute, a quasi-static operating condition is adopted, and the proposed controller is implemented with each iteration updated every 0.2 seconds (a total of 300 iterations per minute).

To validate the performance of the ASDVC in applications, we compare the results with SDVC and ASDVC under random time delays. The maximal time delay is 5s. The profiles of daily network-wide voltage error with ASDVC and SDVC are given in Fig.6. It is illustrated that the voltage deviation with SDVC is bigger than that with ASDVC if there exist time delays. The reason is that each bus under SDVC has to wait for the slowest neighbor to carry out the algorithm. In this situation, it cannot track system changes rapidly. It is different under ASDVC as there is no idling time for each bus. This shows that the ASDVC has better performance in time varying environments when time delays exist.

8. Conclusion

In this paper, we have developed an asynchronous distributed control method to regulate the voltage in distribution networks

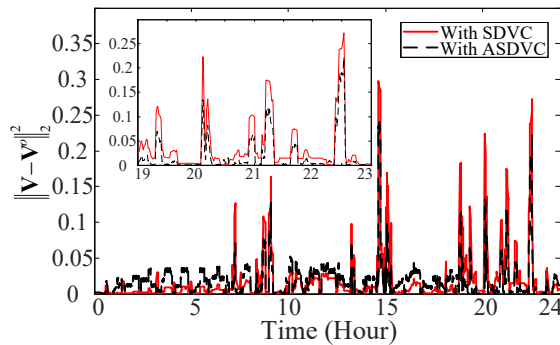


Figure 6: Daily voltage mismatch error with SDVC and ASDVC under random time delays. If SDVC is adopted, every bus has to wait for the slowest one to proceed the iteration. In contrast, every bus can update as long as new information is obtained in the ASDVC.

by making use of both active and reactive controllable power of DERs. The partial primal-dual gradient algorithm is utilized to design the controller with proofs of convergence and optimality of the equilibrium. Finally, numerical tests on an 8-bus system verify the similar convergence speed of SDVC and ASDVC. The daily simulations in the IEEE 123-bus system with real data show that the voltage deviation can be reduced using ASDVC. Simulations under random time delays show that the asynchronous algorithm has better performance in time-varying environments. In the theoretic analysis, the distribution network is assumed to be three-phase symmetric and homogeneous. How to eliminating these restrictions is among our ongoing works.

References

Antoniadou-Plytaria, K.E., Kouveliotis-Lysikatos, I.N., Georgilakis, P.S., Hatzargyriou, N.D., 2017. Distributed and decentralized voltage control of smart distribution networks: models, methods, and future research. *IEEE Trans. Smart Grid* 8, 2999–3008.

Baran, M., Wu, F.F., 1989a. Optimal sizing of capacitors placed on a radial distribution system. *IEEE Trans. Power Delivery* 4, 735–743.

Baran, M.E., Wu, F.F., 1989b. Optimal capacitor placement on radial distribution systems. *IEEE Trans. Power Delivery* 4, 725–734.

Bauschke, H.H., Combettes, P.L., et al., 2011. *Convex analysis and monotone operator theory in Hilbert spaces*. volume 408. Springer.

Bolognani, S., Carli, R., Cavraro, G., Zampieri, S., 2015. Distributed reactive power feedback control for voltage regulation and loss minimization. *IEEE Trans. Autom. Control* 60, 966–981.

Combettes, P.L., Yamada, I., 2015. Compositions and convex combinations of averaged nonexpansive operators. *Journal of Mathematical Analysis and Applications* 425, 55–70.

Farivar, M., Clarke, C.R., Low, S.H., Chandy, K.M., 2011. Inverter var control for distribution systems with renewables, in: *Smart Grid Communications (SmartGridComm)*, 2011 IEEE International Conference on, IEEE. pp. 457–462.

Farivar, M., Neal, R., Clarke, C., Low, S., 2012. Optimal inverter var control in distribution systems with high pv penetration, in: *Power and Energy Society General Meeting, 2012 IEEE*, IEEE. pp. 1–7.

Hale, M.T., Nedić, A., Egerstedt, M., 2017. Asynchronous multiagent primal-dual optimization. *IEEE Trans. Automatic Control* 62, 4421–4435.

Han, Y., Chen, L., Ma, H., Wang, Z., 2014. Optimization of reactive power compensation for distribution power system with small hydro power, in: *Power System Technology (POWERCON)*, 2014 International Conference on, IEEE. pp. 2915–2920.

Kekatos, V., Wang, G., Conejo, A.J., Giannakis, G.B., 2015a. Stochastic reactive power management in microgrids with renewables. *IEEE Trans. Power Syst.* 30, 3386–3395.

Kekatos, V., Zhang, L., Giannakis, G.B., Baldick, R., 2015b. Fast localized voltage regulation in single-phase distribution grids, in: *Smart Grid Com-*

munications (SmartGridComm), 2015 IEEE International Conference on, IEEE. pp. 725–730.

Kekatos, V., Zhang, L., Giannakis, G.B., Baldick, R., 2016. Voltage regulation algorithms for multiphase power distribution grids. *IEEE Trans. Power Syst.* 31, 3913–3923.

Li, N., Zhao, C., Chen, L., 2016. Connecting automatic generation control and economic dispatch from an optimization view. *IEEE Trans. Control Netw. Syst.* 3, 254–264.

Liu, H.J., Shi, W., Zhu, H., 2017. Decentralized dynamic optimization for power network voltage control. *IEEE Trans. Signal Inf. Process. Networks* 3, 568–579.

Liu, H.J., Shi, W., Zhu, H., 2018a. Distributed voltage control in distribution networks: Online and robust implementations. *IEEE Trans. Smart Grid* 9, 6106–6117.

Liu, H.J., Shi, W., Zhu, H., 2018b. Hybrid voltage control in distribution networks under limited communication rates. *IEEE Trans. Smart Grid*.

Meyer, C.D., 2000. *Matrix analysis and applied linear algebra*. volume 71. Siam.

NREL, 2018. Solmap utah geological survey. https://midcdmz.nrel.gov/usep_cedar/.

Peng, Z., Xu, Y., Yan, M., Yin, W., 2016. Arock: an algorithmic framework for asynchronous parallel coordinate updates. *SIAM J. Sci. Comput.* 38, A2851–A2879.

Ruszczynski, A.P., Ruszczyński, A., 2006. *Nonlinear optimization*. volume 13. Princeton university press.

Šulc, P., Backhaus, S., Chertkov, M., 2014. Optimal distributed control of reactive power via the alternating direction method of multipliers. *IEEE Trans. Energy Convers.* 29, 968–977.

Tang, Z., Hill, D.J., Liu, T., 2019. Fast distributed reactive power control for voltage regulation in distribution networks. *IEEE Trans. Power Syst.* 34, 802–805.

Turitsyn, K., Sulc, P., Backhaus, S., Chertkov, M., 2011. Options for control of reactive power by distributed photovoltaic generators. *Proceedings of the IEEE* 99, 1063–1073.

UCI, 2012. Individual household electric power consumption data set. <https://archive.ics.uci.edu/ml/datasets/individual+household+electric+power+consumption>.

Wang, Z., Liu, F., Low, S.H., Zhao, C., Mei, S., 2019. Distributed frequency control with operational constraints, part ii: Network power balance. *IEEE Trans. Smart Grid* 10, 53–64.

Yi, P., Pavel, L., 2019a. Asynchronous distributed algorithms for seeking generalized nash equilibria under full and partial decision information. *IEEE Trans. Cybern., DOI*, 10.1109/TCYB.2019.2908091.

Yi, P., Pavel, L., 2019b. An operator splitting approach for distributed generalized nash equilibria computation. *Automatica* 102, 111–121.

Zhang, B., Lam, A.Y., Domínguez-García, A.D., Tse, D., 2015. An optimal and distributed method for voltage regulation in power distribution systems. *IEEE Trans. Power Syst.* 30, 1714–1726.

Zhou, X., Chen, L., Farivar, M., Liu, Z., Low, S., 2018. Reverse and forward engineering of local voltage control in distribution networks. *arXiv preprint arXiv:1801.02015*.

Zhu, H., Liu, H.J., 2016. Fast local voltage control under limited reactive power: Optimality and stability analysis. *IEEE Trans. Power Syst.* 31, 3794–3803.